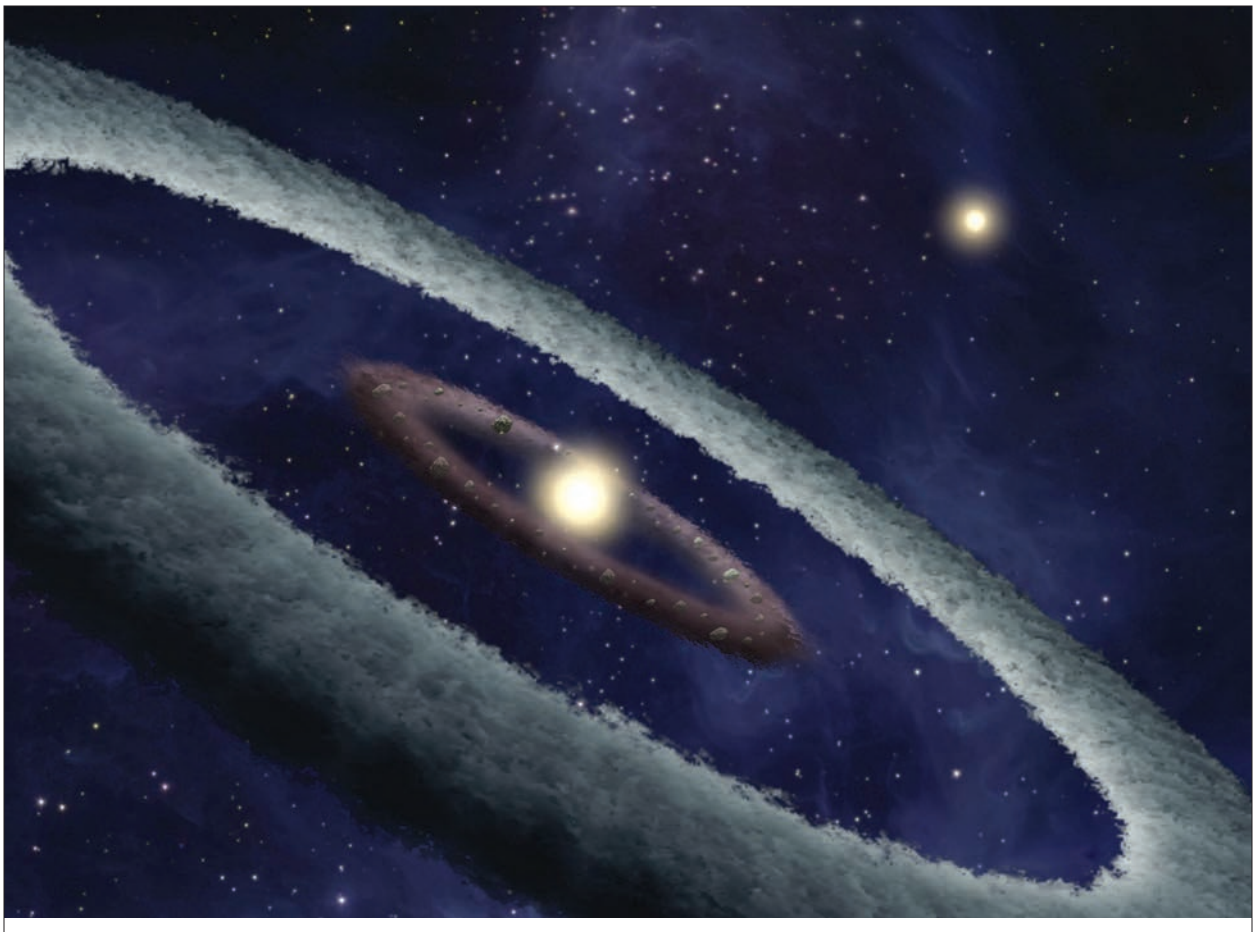

Research Journal of Physics

ISSN 1819-3463

Academic Journals Inc.

www.academicjournals.com

Research Journal of Physics 4 (1): 1-10, 2010
ISSN 1819-3463

Wall and Bed Shear Forces in Open Channels

B. Lashkar-Ara and M. Fathi-Moghadam
School of Water Sciences Engineering, Shahid Chamran University, Ahwaz, Iran

Abstract: The experiments were conducted to evaluate effects of aspect ratio on wall and bed shear forces in rectangular channels. The objective was to determine contribution of wall shear force on total boundary shear force. A Preston tube connected to a differential pressure transducer and a data acquisition system was used to measure velocity heads at channel wall and bed. The calibration curves proposed by Patel were used to convert the pressure readings to shear stress. The results were adjusted by the total shear force calculated from the energy method. A nonlinear regression-based technique was carried out to analyze the results and develop equations to determine the percentage of wall and bed shear force on the wetted perimeter of rectangular channels. The proposed equations were compared and well correlated with previous studies. The new data has significant contribution on understanding and development of new relationships for boundary shear force.

Key words: Shear force, preston tube, open channel

INTRODUCTION

Flowing of water channels, a force in flow direction is developed on the channel bed and walls. The reaction of this force which pulls the flow body is known as tractive force. The flow structure in an open channel is directly affected by the shear stress distribution along the wetted perimeter. It is difficult to determine boundary shear distributions in real life applications. Laboratory flume studies have still been serving to cope with this difficulty.

The problem of separating the bed shear stress and the side-wall shear stress is very important in most open-channel flow studies. For example, in order to estimate the amount of bed load, the wall shear stress should be subtracted from the total shear stress. Similarly, for estimation of erosion in sea coast and river levees, wall shear stress must be known. Since, the 1960s, several experimental studies have been reported for measurement of boundary shear stresses in rectangular open channels with different aspect ratios (Knight, 1981; Knight *et al*., 1984). Similar works were conducted later to evaluate effect of sidewalls on bed shear stress and to reconfigure previous relationship for estimation of the sidewall corrected bed shear stress in open channel flow (Cheng and Chua, 2005; Seckin *et al*., 2006). For the pipe flow, Berlamont *et al.* (2003) studied boundary shear stress in partially filled pipes with high wetted perimeter and hydraulic radius. An analytical approach by Guo and Julien (2005) revealed considerable effect of sidewall on generation of eddy viscosity and secondary currents and their effects on bed shear stress. Recently, Khodashenas *et al.* (2008) presented a comparison between verities of methods developed for boundary shear

Corresponding Author: M. Fathi-Moghadam, School of Water Sciences Engineering, Shahid Chamran University, Ahwaz, Iran
Tel: +98-611-3738359 Fax: +98-611-3365678

stress in open channel flow. Results of these shear studies support the understanding of turbulent boundary layer flow and computation of velocity profile for open channel flows (e.g., Tang and Knight, 2009).

In spite of the completed work on open channel flow, more shear stress measurements on different flow and boundary conditions are required to validate results and put them into practice. The purpose of this study is to determine contribution of wall and bed shear force on total boundary shear in a relatively wider rectangular channel. That experiments were conducted in a 25% larger channel than have ever been used with aspect ratios around 6-19. A set of nonlinear regression-based equations were developed for estimation of percentage of wall and bed shear force and shear velocity in wider channels and larger aspect ratios.

MATERIALS AND METHODS

Theory

Knight *et al.* (1984) used 43 data points for range 0.3<B/H and 12 data points for 6<B/H to correlate following dimensionless log-relationship for percentage of wall shear force

$$SF_w(\%) = \text{Exp}\,(-3.23\times\log\,(B/H+3)+6.146) \quad (1)$$

where, SF_w is the percentage of the shear force acting on the channel walls; B is the width of the channel; H is the flow depth.

Using the energy principle for unit width of channel (a two dimensional analysis), the dimensionless mean value of wall and bed shear stresses were expressed as:

$$\frac{\overline{\tau}_w}{\rho g H S_f} = 0.01\times \%SF_w \times \left(\frac{B}{2H}\right) \quad (2)$$

$$\frac{\overline{\tau}_b}{\rho g H S_f} = 1 - 0.01\times \%SF_w \quad (3)$$

where, $\overline{\tau}_w$ and $\overline{\tau}_b$ are the mean wall and bed shear stresses, respectively; ρ is fluid density; g is gravitational acceleration, S_f is the energy gradient.

Since, application of bed shear velocity ($\overline{u}_{*b} = \sqrt{\overline{\tau}_b/\rho}$) is more common in practice of open channel flow, using Eq. 2, the dimensionless bed shear velocity will be.

$$\frac{\overline{u}_{*b}}{\sqrt{g H S_f}} = (1 - 0.01\times \%SF_w)^{1/2} \quad (4)$$

In addition, the mean wall and bed shear stresses may be presented in dimensionless forms using the mean overall boundary shear stress ($=\rho g R S_f$).

$$\frac{\overline{\tau}_w}{\rho g R S_f} = 0.01\times \%SF_w \times \left(1 + \frac{B}{2H}\right) \quad (5)$$

$$\frac{\overline{\tau}_b}{\rho g R S_f} = (1 - 0.01\times \%SF_w)\left(1 + \frac{2H}{B}\right) \quad (6)$$

in which R is hydraulic radius.

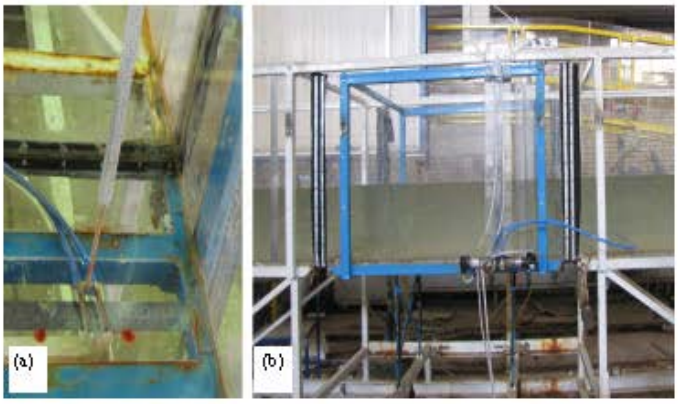

Fig. 1: (a) Experimental flume and Preston tube, (b) pressure transducer

Experimental Set up

The experiments were conducted in 2009 at the Hydraulic Modeling Laboratory of the School of Water Sciences and Engineering of Shahid Chamran University of Ahwaz, Iran. A rectangular flume 8.6 m long, 80 cm wide and 55 cm height was constructed for the experiments. The boundary shear stresses were measured all around the wetted perimeter of the Plexiglas flume using a Preston tube (4-mm outside diameter, Fig. 1). All measurements were conducted in a constant hydraulic gradient of 1.05×10^{-3} at mid section of the flume where flow was uniform and fully turbulent. Dynamic and static pressures were recorded using a differential pressure transmitter (Model: Dwy-PT616) with a pressure range of ±76 mm of water, accuracy of 0.25% and stability of 1%. An analog/digital signal converter (Model: RL-PAXP) was used to produce compatible pressure signals for computer and data acquisition software. A frequency of 10 s^{-1} and period of 2 min was assigned for collection of data in every run of experiments. The time average of the collected data was incorporated in analyses of wall and bed shear stresses. Velocities were measured with a Nixon probe micro-propeller and were checked with a sharp V-notch weir down stream of the water circulating system. The flow depths varying from 4.3 and 13.3 cm were measured using a precision point gage with accuracy of 0.1 mm.

Shear stresses were measured at intervals of 1 to 5 cm around the wetted perimeter and shear stress distribution curves were drawn. The area under the curves was measured for wall and bed mean shear forces. The calibration curves of Patel (1965) were used to convert pressure readings to boundary shear stresses. Patel (1965) conducted further experiments than those by Preston (1954) in order to produce reliable and definitive calibration curves for converting pressure readings to the shear stress as follow:

$$y^* = 0.5x^* + 0.037 \text{ for } 0 < y^* < 1.5 \quad (7)$$

$$y^* = 0.8287 - 0.1381x^* + 0.1437x^{*2} - 0.006x^{*3} \text{ for } 1.5 < y^* < 3.5 \quad (8)$$

$$x^* = y^* + 2\log(1.95y^* + 4.1) \text{ for } 3.5 < y^* < 5.3 \quad (9)$$

Where:

$$x^* = \log\left(\frac{\Delta P\, d^2}{4\rho\upsilon^2}\right) \tag{10}$$

$$y^* = \log\left(\frac{\tau_o d^2}{4\rho\upsilon^2}\right) \tag{11}$$

in which, ΔP is Preston tube differential pressure (dynamic pressure), d is the outside diameter of the probe, ρ is fluid density, υ is kinematic viscosity, τ^o is overall boundary shear stress; y^* is the logarithm of the dimensionless shear stress; x^* is logarithm of the dimensionless pressure difference.

Since, then the calibration equations have widely been used for measurement of boundary shear stresses in smooth and rough open channels.

RESULTS AND DISCUSSION

Using Patel's calibration equations for the Preston tube pressure readings in this study, the local bed and wall shear stresses and forces were calculated in Table 1 for different discharges through the channel at constant pressure gradient of 2.00×10^{-3}. The numerically integrated shear stress distributions were used to calculate the bed and wall shear forces per unit length of the channel. Percentage of the measured wall shear force to the total boundary shear force for different ratio of B/H is shown in Table 2. Using the left hand side of Eq. 2 to 6, dimensionless wall and bed shear stresses and shear velocity are also calculated in Table 2.

The percentage of wall shear force in Table 2 against aspect ratio is shown in logarithm and natural scales in Figs. 2 and 3, respectively. Data sets from Seckin *et al.* (2006) and other sources (Knight *et al*., 1984; Knight, 1981) are also shown on the figures. The data set in this study falls well among the other data sets in Fig. 2 and 3. Incorporating experimental results of this study and the data set of Seckin *et al.* (2006), Eq. 1 (developed by Knight *et al*., 1984 based on his previous studies) is adjusted using linear regression of the logarithmic scale of %SFw against B/H+3 in Fig. 2, and the proposed equation is as follow,

$$\%SF_w = \exp(-3.238\times\log(B/H+3)+6.171) \tag{12}$$

Table 1: Wall and bed shear stresses measurements

Water depth H (mm)	B/H	Discharge Q (L sec^{-1})	Velocity V (m sec^{-1})	Shear stress (N m^{-2}) $\bar{\tau}_b$	Shear stress (N m^{-2}) $\bar{\tau}_w$	Shear force (N) Sf_W	Shear force (N) SF_W	Shear force (N) SF_P
0.101	7.96	69.62	0.866	1.570	1.239	1.256	0.249	1.505
0.095	8.42	65.47	0.861	1.564	1.222	1.251	0.232	1.483
0.081	9.94	50.55	0.785	1.328	1.024	1.063	0.165	1.228
0.075	10.67	44.91	0.749	1.285	0.928	1.028	0.139	1.167
0.071	11.27	41.18	0.725	1.214	0.868	0.971	0.123	1.094
0.062	12.90	33.28	0.671	1.058	0.745	0.847	0.092	0.939
0.059	13.56	31.03	0.657	1.033	0.722	0.827	0.085	0.912
0.056	14.29	28.63	0.639	0.987	0.682	0.790	0.076	0.866
0.053	15.01	26.55	0.623	0.921	0.647	0.737	0.069	0.806
0.049	16.33	22.77	0.581	0.858	0.562	0.687	0.055	0.742
0.047	17.02	21.49	0.571	0.840	0.545	0.672	0.051	0.723
0.046	17.39	20.74	0.564	0.812	0.536	0.649	0.049	0.699
0.045	17.78	20.00	0.556	0.799	0.521	0.639	0.047	0.686
0.043	18.60	18.33	0.533	0.773	0.478	0.618	0.041	0.660

Table 2: Dimensionless wall and bed shear stresses and bed shear velocity

B/H	Percentage shear force on walls % Sfw	Mean wall shear stress $\overline{\tau}_w / \rho g H S_f$	Mean bed shear stress $\overline{\tau}_b / \rho g H S_f$	Mean wall shear stress $\overline{\tau}_w / \rho g R S_f$	Mean bed shear stress $\overline{\tau}_b / \rho g R S_f$	Mean bed sheare locity $\overline{u}_{*b} / \sqrt{gHS_f}$
7.96	16.55	16.55	0.817	0.807	1.022	0.904
8.42	15.65	15.65	0.861	0.832	1.065	0.928
9.94	13.43	13.43	0.863	0.799	1.037	0.929
10.67	11.93	11.93	0.896	0.768	1.064	0.946
11.27	11.26	11.26	0.894	0.752	1.053	0.946
12.9	9.84	9.84	0.893	0.726	1.031	0.945
13.56	9.34	9.34	0.916	0.734	1.051	0.957
14.29	8.82	8.82	0.922	0.726	1.051	0.960
15.01	8.56	8.56	0.904	0.72	1.024	0.951
16.33	7.43	7.43	0.916	0.674	1.028	0.957
17.02	7.08	7.08	0.935	0.678	1.045	0.967
17.39	7.05	7.05	0.923	0.679	1.029	0.961
17.78	6.83	6.83	0.928	0.673	1.032	0.963
18.6	6.23	6.23	0.940	0.644	1.041	0.970

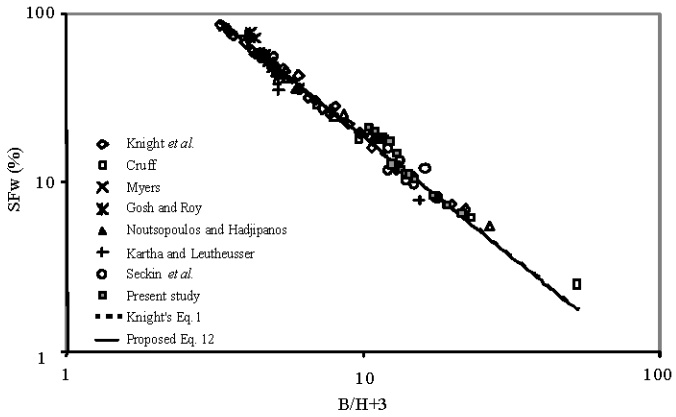

Fig. 2: Percentage of wall shear force versus B/H+3

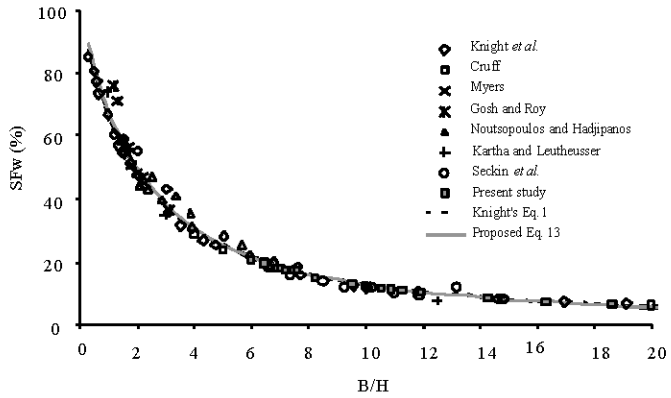

Fig. 3: Percentage of wall shear force versus B/H

In addition, a nonlinear regression of the percentage of wall shear force (%SFw) and the channel aspect ratio (B/H +3) for all measurements in Fig. 3 produces the following equation,

$$\%SF_w = 478.5\left(\frac{B}{H}+3\right)^{-1.406} \tag{13}$$

To be consistent with previous studies, the dimensionless wall and bed shear data sets reported in Knight *et al.* (1984) were re-correlated incorporating the experimental data set of this study and the Seckin *et al.* (2006) data set. The results are compared with Knight's correlation Eq. 2 to 6 in Fig. 4-8. The proposed correlated equations are as follows:

$$\frac{\overline{\tau}_w}{\rho g H.S_f} = \frac{0.833\times(B/H)-0.115}{1+1.057\times(B/H)+0.0125\times(B/H)^2} \tag{14}$$

$$\frac{\overline{\tau}_b}{\rho g H.S_f} = \frac{1.0166\times(B/H)^{1.1254}}{2.2415+(B/H)^{1.1254}} \tag{15}$$

$$\frac{\overline{u}_b}{\sqrt{g H.S_f}} = \frac{0.5065+1.0048\times(B/H)^{1.1677}}{1.6772+(B/H)^{1.1677}} \tag{16}$$

$$\frac{\overline{\tau}_w}{\rho g R S_f} = \frac{0.0113}{1-0.9893\times\exp[-0.0004(B/H)]} \tag{17}$$

$$\frac{\overline{\tau}_b}{\rho g R S_f} = \frac{0.9383+0.3326(B/H)}{1+0.2995(B/H)+0.00074(B/H)^2} \tag{18}$$

In general, the data sets were best fit with the Sigmoidal-Hill Eq. 3 Parameter and the Rational-4 Parameter models.

The experimental measurements of wall and bed shear forces in Fig. 2 and 3 reveal considerable effect of aspect ratio (B/H) on percentage of wall shear force. The contributions of wall shear force to total boundary shear decreases by 10 fold when the aspect ratio increases from 1 to 20 in Fig. 3. A two dimensional approach for normalization of the wall and bed shear stresses in Fig. 4 and 5 demonstrates a rapid growth of both wall and bed shear stresses in small aspect ratios, while the curves have stagnated in aspect ratio around 6 and

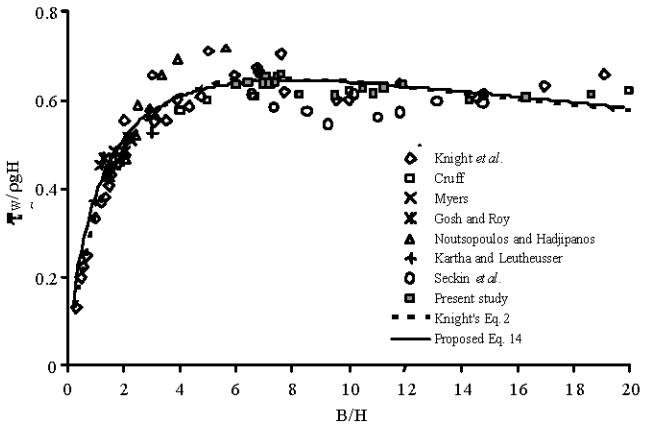

Fig. 4: Dimensionless mean wall shear stress versus B/H, (2D analysis)

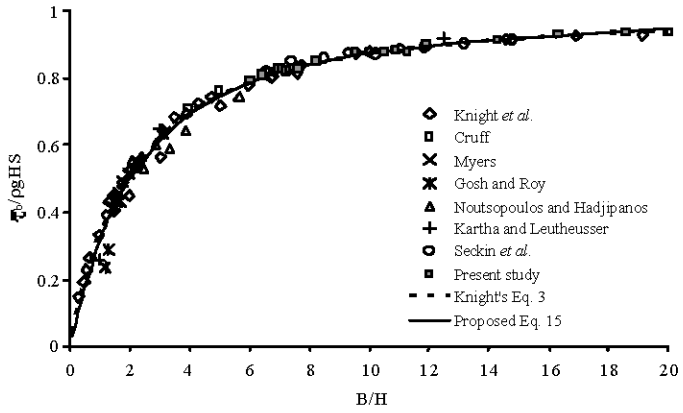

Fig. 5: Dimensionless mean bed shear stress versus B/H, (2D analysis)

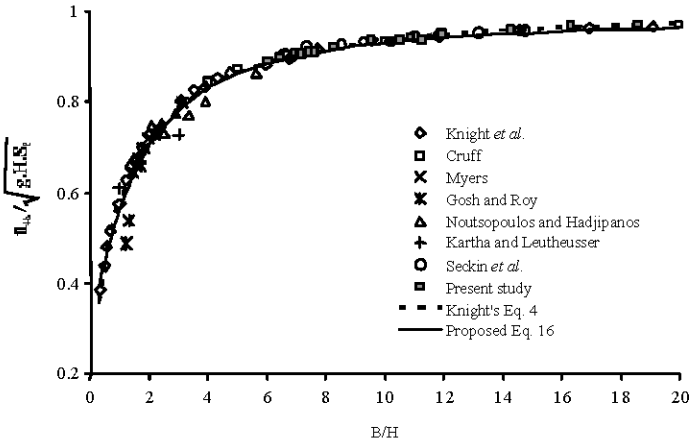

Fig. 6: Dimensionless mean bed shear velocity versus B/H, (2D analysis)

follow a decrease with increasing aspect ratio. Similar results are reported in Fig. 6 for the bed mean shear velocity. However, normalization of the wall and bed shear stresses with hydraulic radius (i.e., a 3-dimensional analysis) granted more correct results in Fig. 7 and 8. Figure 7 shows a reasonable decrease of the mean wall shear stress with increase of aspect ratio. For the bed shear stress in Fig. 8, the effect of aspect ratio ore than 6 does not affect wall shear contribution.

In lower aspect ratios, a two dimensional normalization of the wall and bed shear stresses and shear velocity with flow depth (H) demonstrates a rapid growth of the parameters with aspect ratios (Fig. 4-6), while the effect is insignificant for aspect ratios more than 6. However, normalization of the wall and bed shear stresses with hydraulic radius (i.e., a 3-dimensional analysis) improved the results considerably. In this case increase of aspect ratio causes a moderate reduction of average wall shear stress (Fig. 7), while was ineffective on the average bed shear stress (Fig. 8).

The results of this study for contribution of wall and bed shear stresses and shear forces are well agreed with previous studies. The statistical results of correlation of the proposed equations for wall and bed shear stresses and forces (Eq. 12-18) are compared with the

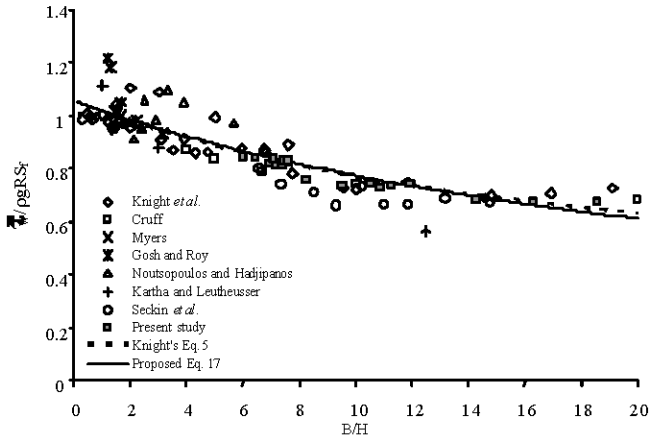

Fig. 7: Dimensionless mean wall shear stress versus B/H, (3D analysis)

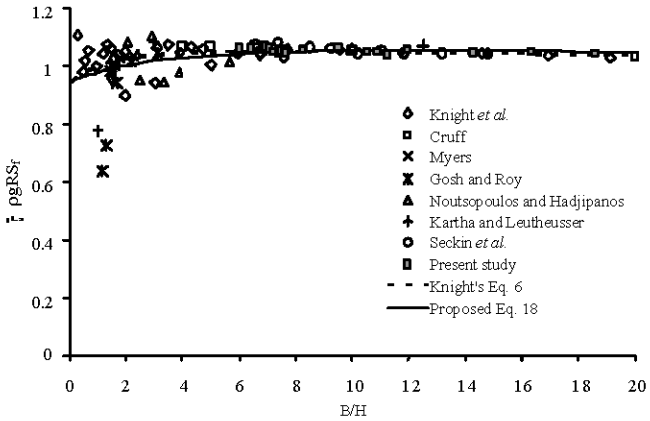

Fig. 8: Dimensionless mean bed shear stress versus B/H, (3D analysis)

Table 3: Statistical results of correlation for equations proposed by Kight *et al.* (1984) and current study

Knight *et al.* (1984) Eq.			Proposed Eq. (current study)		
Eq. No.	R^2	SD	Eq. No.	R^2	SD
1	0.985	21.31	12	0.987	21.20
1	0.985	21.31	13	0.988	21.20
2	0.849	0.117	14	0.846	0.115
3	0.985	0.210	15	0.985	0.220
4	0.943	0.142	16	0.947	0.142
5	0.740	0.132	17	0.772	0.121
6	0.137	0.028	18	0.162	0.018

Knight's correlation equations (Eq. 1-6) in Table 3. The results are very close with some improvement particularly for wall and bed shear stresses equations.

CONCLUSIONS

Results of a 2-D analysis confirm considerable effect of aspect ratio (B/H) on percentage of wall shear force. The contribution of wall shear force on total boundary shear decreases

rapidly as the aspect ratio increases particularly at low aspect ratios. A same track is also observed for wall shear stress at high aspect ratio. However, in aspect ratio less than 6, a growth in wall shear is recorded due to the increase of relative flow velocity with increasing the flow depth. In contrast, a result for application of the hydraulic radius instead of flow depth in form of a 3-D analysis confirms the ability of hydraulic radius to cover variations in wall shear contribution with aspect ratio.

The proposed equations in this study (Eq. 12-18) can estimate wall and bed shear forces and stresses as well as shear velocity as long as channel geometry (B and H), and slope (S_f) are known. The equations are valid for subcritical and supercritical flows while a uniform channel flow can be assumed. Direct correlation of shear stress and shear velocity with aspect ratio is the advantages of the proposed equations over previous equations that depend on the percentage of wall shear force ($\%SF_w$) as well as the aspect ratio.

ACKNOWLEDGMENT

The authors acknowledge Shahid Chamran University of Ahwaz, Iran for financial support of the research (Grant No. 696). The authors are also acknowledging Farzad Shamshiri and Kad Controls Co., Tehran, Iran for their technical assistant.

NOTATIONS

B = Channel width
g = Gravitational acceleration
H = Channel depth
P = Wetted perimeter
Q = Flow Discharge
R = Hydraulic radius
SD = Standard Deviation
S_f = Energy gradient
SF = Shear force
%SF = Percent shear force
$\overline{u}_{*b}$ = Mean bed shear velocity
V = Section mean velocity obtained from the weir
ρ = Density
τ = Local shear stress
$\overline{\tau}$ = Mean shear stress
$\overline{\tau}_e$ = Mean boundary shear stress calculate by
$\overline{\tau}_o$ = Measured mean boundary shear stress

REFERENCES

Berlamont, J.E., K. Trouw and G. Luyckx, 2003. Shear stress distribution in partially filled pipes. J. Hydr. Eng., 129: 697-705.

Cheng, N.S. and L.H.C. Chua, 2005. Comparisons of sidewall correction of bed shear stress in open-channel flows. J. Hydr. Eng., 131: 605-609.

Guo, J. and P.Y. Julien, 2005. Shear Stress in smooth rectangular open-channel flows. J. Hydr. Eng., 125: 30-37.

Khodashenas, S.A., K.E. Abderrezzak and A. Paquier, 2008. Boundary shear stress in open channel flow: A comparison among six methods. J. Hydr. Res., 46: 598-609.

Knight, D.W., 1981. Boundary shear in smooth and rough channels. J. Hydr. Div., 107: 839-851.

Knight, D.W., J.D. Demetriou and M.E. Homed, 1984. Boundary shear in smooth rectangular channels. Agric. Water Manage., 110: 405-422.

Patel, V.C., 1965. Calibration of the Preston Tube and limitations on its use in pressure gradients. J. Fluid Mech., 23: 185-208.

Preston, J.H., 1954. The determination of turbulent skin friction by means of pitot tubes. J. Roy. Aero. Soc. 58: 109-121.

Seckin, G., N. Seckin and R.G. Yurtal, 2006. Boundary shear stress analysis in smooth rectangular channels. Can. J. Civ. Eng., 33: 336-342.

Tang, X. and D. Knight, 2009. Analytical models for velocity distributions in open channel flows. J. Hydr. Res., 47: 418-428.